Recovery of niobium and tantalum from tin slags: An alternative approach using acid roasting and oxalic leaching

Darwin Michell Cheje Machaca [a,*], Rosario Belen Juyo Salazar [a],
Thamyres Cardoso de Carvalho [b], Denise Crocce Romano Espinosa [a],
Jorge Alberto Soares Tenório [a]

[a] *Department of Chemical Engineering, University of Sao Paulo, São Paulo, Brazil*
[b] *Department of Chemical Engineering, Fei University, São Paulo, Brazil*

A B S T R A C T

An alternative approach for extracting Nb and Ta was investigated, based on the acid roasting of tin slags using the $KHSO_4$-H_2SO_4 system, followed by oxalic leaching. Roasting experiments demonstrated the formation of soluble sulfated products, optimized through thermodynamic modeling: mineral grain size fraction -75 μm, Slag-$KHSO_4$-H_2SO_4 ratio 1:0.5:0.5 (g:g:ml), roasting temperature 300 °C, and roasting time 2 h. Under these conditions, the material conversion rate was maximized, characterized by mineralogical and morphological analyses that showed the chemical changes occurring during roasting helped explain the mechanisms at work during the process. After optimizing the treatment parameters by varying process conditions, it was found that approximately 94 % of Nb and 75 % of Ta were dissolved during the oxalic leaching stage, under the following conditions: concentration 0.5 mol L^{-1}, S/L ratio 50 g L^{-1}, reaction temperature 60 °C for 60 min. Consequently, this innovative alternative could reduce reagent and energy consumption, promoting a sustainable approach with a lower environmental footprint.

1. Introduction

The cassiterite is the main Sn mineral and contributes about 78.6 % of global production (Dutta & Lodhari, 2018), holding critical and strategic importance in developing of modern society for different nations (Calvo & Valero, 2022). The metallurgical processing of cassiterite involves a series of stages that generate ferrous, non-ferrous, and incineration by-products after beneficiation to obtain a primary product (Shen & Forssberg, 2003; G. C. Wang, 2016). In this context, the tin slags obtained after a reduction process with carbon at temperatures above 1000 °C are characterized by the concentration of elemental phases in the form of oxides (Table 1) within the interatomic networks of the produced slags (Clemente et al., 2023; Dutta & Lodhari, 2018).

In Table 1, metals of high economic interest, such as Nb and Ta, are highlighted for their intrinsic properties of corrosion resistance, mechanical strength, and thermal shock resistance, which are applied in various industrial sectors, including electronics, nuclear, steel, and high technology (Cheje Machaca et al., 2025). Despite the importance of these metals, they are defined as critical metals due to the risks in their supply chains for the USA and the EU (DOE, 2023; European Commission, 2023); while they are strategic materials for the development of new technologies in Brazil (Pope & Smith, 2023).

With the recent high demand for niobium and tantalum, attention is increasingly focused on reprocessing mining waste and slag dumps to recover the associated oxides. Conventional methods for the disposal of these secondary wastes involve dumping them over large areas of land, resulting in impacts on the management of these wastes (Shen & Forssberg, 2003). It is documented that the disposal of these materials across different territories has varied over the decades, depending on the characteristics of the mineral. For example, in Canada, around 2 Mt of slag are disposed of (Mikhail & Webster, 1992), while in Brazil, approximately 600,000 t are estimated (Garcia, 2009). In Malaysia, an estimated 20,000 to 24,000 tons per year of tin slags are disposed of (Abd & Yusof, 2005). Currently, there is no statistical data on the disposal of these wastes, but it is known that in 2023, the global mining waste market reached 209.5 Mt, with an expected total volume of 308.9 Mt by 2032, growing at a rate of 4.4 % globally (Research and Markets, 2024). Given the availability of these materials, it is necessary to promote the need to add value to secondary raw material chains that contain economically valuable metals.

The economic approach for the recovery of both tantalum and niobium from slags is focused on acid leaching based on a mixture of HF or thermal processes of their derivatives and leaching in highly acidic media (Anes et al., 2023; Rodríguez et al., 2020; Xie et al., 2022). However, the operability of the process is hindered mainly by the environmental problems caused by F$^-$ ions, posing operational challenges in the industrial-scale production of Nb and Ta (Cheje Machaca et al., 2025). Very few detailed studies have been reported on the pyrometallurgical and hydrometallurgical recovery of both metals from tin slags (Table 2).

Despite the studies on the recovery of Nb and Ta, there is virtually no systematic, fundamental, and applied approach to extracting both metals. While it is true that the proposed methodologies offer alternatives for metal recovery, operational challenges persist in the industrial-scale production of Nb and Ta from secondary waste.

In recent decades, alternative processes to direct acid leaching based on combining pyrohydrometallurgical methods have been increasingly adopted (Kim & Azimi, 2020). In these processes, minerals/wastes are mixed with highly concentrated acids and roasted in furnaces at temperatures above 100 °C. Subsequently, the roasted materials are leached with water or organic reagents under atmospheric pressure and temperature conditions (<100 °C) (Kim & Azimi, 2020). Although research studies employing these processes are limited to tin slags, unsuccessful attempts have been reported. For example, (J. M. de Oliveira, 2022) adopted acid roasting and sulfuric leaching to extract niobium and Ta from tin slags, achieving 40 % Nb and 35 % Ta extractions. In contrast, after an alkaline fusion process and sulfuric leaching, the extraction of Nb was above 90 %. (Conrado Da Luz, 2023) After an alkaline fusion process, complexing the material with oxalic acid enhanced the results, obtaining 86 % Nb and 75 % Ta using more sequential steps.

This research introduces an alternative for the recovery of Nb and Ta, eliminating the need for hydrofluoric acid based on the KHSO$_4$–H$_2$SO$_4$ roasting system and oxalic leaching from tin slags. This production method provides a perspective on the management and control of optimal working conditions through thermodynamic modeling in the roasting process, leading to increased profitability due to reduced processing steps. Furthermore, during oxalic acid leaching, the effects of solid–liquid ratio, concentration, time, and temperature were thoroughly analyzed to provide the necessary foundations for future industrial application.

2. Materials and methods

2.1. Materials

This research received 120 kg of tin slag sourced from a carbothermic process of cassiterite in Brazil. The material was dried, homogenized, and quartered. A representative sub-sample was collected for characterization and sieved using a set of standard ASTM sieves, which showed a particle size of 0.811 mm. The material was then comminuted in a HERZOG-brand pulverizer, using a 0.075 mm sieve. Sulfuric acid, potassium bisulfate, and oxalic acid in analytical grade were used as roasting and leaching agents. Additionally, Milli-Q water < 0.05 µS·cm − 1 and ultrapure water (> 18 MΩ·cm, Milli-Q-POD) were used for solution preparation and residue washing.

2.2. Characterization

The mineralogical composition of the study material was analyzed by collecting X-ray diffraction (XRD) data using a Rigaku diffractometer (model MiniFlex300) in the 2θ range of 20°–80°. The chemical analysis of the slag was quantitatively performed using ICP-OES (Agilent, model 710 series), AAS (Shimadzu, model AA7000), and EDXRF (PANalytical, model Epsilon 7200) to determine the Nb and Ta contents in the original sample. The microstructural characterization of the phases present in the tin slag was carried out using a scanning electron microscope (SEM) (Phenom, model ProX), and for the roasted material and the leaching residues, a SEM (JEOL, model JCM-7000) coupled with an energy-dispersive X-ray spectroscopy (EDS) system was used. Likewise, the solid products obtained from roasting and leaching were analyzed using a wavelength-dispersive X-ray fluorescence (WDXRF) instrument (Shimadzu, model XRF-1800), with a methane and argon gas flow.

2.3. Experimental procedure

2.3.1. Theoretical reaction mechanisms of the process

It has been reported that the decomposition reaction of potassium bisulfate and sulfuric acid begins at temperatures above 300 °C, as shown in Eqs. 1, 2, 3, and 4 (T. F. de Oliveira et al., 2020; Zhang et al., 2014).

$$2KHSO_4 \rightarrow 2\,K^+ + 2HSO_4^- \tag{1}$$

$$2HSO_4^- \rightarrow S_2O_7^{2-} + H_2O \tag{2}$$

$$H_2SO_4 \rightarrow H_2O + SO_3\uparrow \tag{3}$$

Table 1
Distribution of oxidized phases in different slags (.

Slag type	2nd slag (wt%)	Slag F (wt%)	Slag "waste 2008″ (wt%)	Ground final slag (wt%)	1st slag (wt%)	1st slag (wt%)	Slag (wt%)
Source	(Clemente et al., 2023)	(Brocchi & Moura, 2008)	(Garcia, 2009)	(Clemente et al., 2023)	(López et al., 2018)	(Permana et al., 2020)	(Conrado Da Luz, 2023)
SnO$_2$	0.1–1.12	–	1.5	6.1	5.66	22.95	3.41
SiO$_2$	25	27.0	33.2	28.7	10	11.34	36.58
CaO	22	9.6	12.8	22.4	15.8	NA$^{(b)}$	14.76
Fe$_2$O$_3$	12$^{(a)}$	6.2	4.53	6.0$^{(a)}$	0.73	14.72	5.7
ZrO$_2$	5.5	19.2	16.7	15.7	3.68	2.41	10.4
Nb$_2$O$_5$ + Ta$_2$O$_5$	6	7.4–1.4	7.6–1.62	5.5 + NA$^{(b)}$	21.4 + 25.4	0.58–0.29	6 + 0.65
Al$_2$O$_3$	10	7.4	3.1	3.1	3.23	4.48	4.26
TiO$_2$	10	6.2	1.76	2.0	0.62	4.92	1.03
MgO	6	2.7	0.94	1.6	0.14	–	4.16
MnO	0.01–0.1	–	0.97	–	7.23	–	0.56
P$_2$O$_5$	2	–	0.06	–	–	–	–
ThO$_2$	1.3	–	5.7	–	–	–	2.0
Other oxides	0.01–1.0	–	9.86	8.9	0.81	–	5.6

Note: (a) wt% calculated as FeO and **(b)** information not available.
Adapted from (Clemente et al., 2023))

Table 2

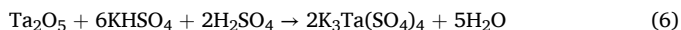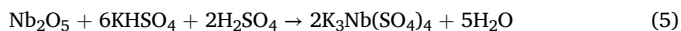Nb and Ta extraction processes from tin slags (.

Material	Conditions Pyrometallurgical	Hydrometallurgical	Results (wt%) Nb	Ta	Source
Tin slag	–	80 °C, 3–6 h, (unspecified)	7.5[(a)]	8.4[(b)]	(Brocchi & Moura, 2008)
Tin slag	Roasted 800 °C, 1 h	NaOH 5 mol L^{-1} 20 min HCl 5 mol L^{-1} 50 min	1.11[(a)]	1.56[(b)]	(Soedarsono et al., 2018)
Tin slag	Roasted 900 °C, 2 h	NaOH 8 mol L^{-1}, ratio L/S (10:1), 2 h, 25 °C	0.76	0.18	(Akli et al., 2019)
		H$_3$PO$_4$ 0.5, 1, and 1.5 mol L^{-1}, ratio L/S (10:1), 2 h, 25 °C	1.45	0.8	
Tin slag	–	NaOH 8 mol L^{-1}, HClO$_4$ 0.8 mol L^{-1}, ratio L/S (10:1) 2 h, 25 °C	1.28	0.8	(Vincia et al., 2019)
Ting slag	–	HCl 2 mol L^{-1}, HF 1.2 mol L^{-1}, NaOH 2 mol L^{-1}, 4 h, 70 °C, Solids 50 g/L	63[(c)]		(Allain et al., 2019)
Tin slag	Roasted 900 °C, 2 h	HCl 6 mol L^{-1}, 65 °C (unspecified)	3.57[(a)]	3.75[(b)]	(Permana et al., 2020)
Ting slag	H$_2$SO$_4$-slag, ratio w/v (1:1) 200 °C, 2 h	H$_2$SO$_4$ 2 mol L^{-1}, ratio L/S (20:1), 2 h, 90 °C	40	35	(J. M. de Oliveira, 2022)
Ting slag	NaOH-slag, ratio w/w (1:1) 700 °C, 3 h	H$_2$SO$_4$ 10 mol L^{-1}, ratio L/S (30:1), 2 h, 90 °C	93	2	(J. M. de Oliveira, 2022)
Tantalum slag	NaOH basicity 40 wt%, ratio L/S (4:1), 200 °C, 2 h, 2 MPa	HF 10 mol L^{-1}, ratio L/S (5:1), 60 °C, 1 h	95.42	93.62	(Xie et al., 2022)
Ting slag	NaOH, ratio w/w (1:1,1), 500 °C, 2 h	H$_2$C$_2$O$_4$ 1 mol L^{-1}, ratio L/S (10:1), 25 °C, 30 min, 240 rpm	86	75	(Conrado Da Luz, 2023)
Ting slag	–	0.12 g NH$_4$F, HCl 30 %, ratio L/S (20:1), 85 °C, 4 h	100	5	(Anes, 2023)

Note: (a) wt. % as Nb$_2$O$_5$, **(b)** wt. % as Ta$_2$O$_5$, **(c)** wt. % by weight (Ta + Nb)$_2$O$_5$.
Adapted from (Cheje Machaca et al., 2025))

$$SO_3 \rightarrow SO_2 + 1/2O_2 \tag{4}$$
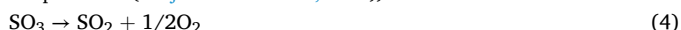
In this study, the roasting system temperature was primarily maintained at 300 °C, resulting in sulfation reactions in the (Nb, Ta)$_2$O$_5$-KHSO$_4$-H$_2$SO$_4$ system, as shown in Eqs. 5 and 6 (Gao et al., 2021).

$$Nb_2O_5 + 6KHSO_4 + 2H_2SO_4 \rightarrow 2K_3Nb(SO_4)_4 + 5H_2O \tag{5}$$

$$Ta_2O_5 + 6KHSO_4 + 2H_2SO_4 \rightarrow 2K_3Ta(SO_4)_4 + 5H_2O \tag{6}$$

It is evident that in Eqs. 5 and 6, is not only temperature a key factor but also the involvement of factors such as time and the mass ratio of agents to the material under study, as previously investigated in the literature (Cheje Machaca et al., 2025; Gao et al., 2014, 2021; Wu et al., 2014). In this study, the influencing parameters during the leaching tests were systematically investigated with the strategy of maximizing metal recovery from the sulfation products. In this stage, the complexation reactions of the sulfation products are presented in Eqs. 7 and 8 (Cheje Machaca et al., 2025; Gao et al., 2021).

$$Nb_2O_3(SO_4)_2 + 6H_2C_2O_4 \rightarrow 2H_3[NbO(C_2O_4)_3] + 2H_2SO_4 + H_2O \tag{7}$$

$$Ta_2O_3(SO_4)_2 + 6H_2C_2O_4 \rightarrow 2H_3[TaO(C_2O_4)_3] + 2H_2SO_4 + H_2O \tag{8}$$
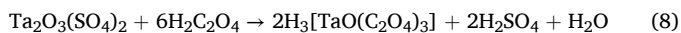
2.3.2. Thermodynamic simulation

Equilibrium reactions for each solid, liquid, and gas phase were studied using HSC Chemistry v6 software, utilizing the ab initio databases (sulfate database) calculated from Fact*Sage* v8.3 software (Cheje Machaca et al., 2025). Through this software, phase equilibrium predictions and thermochemical reactions were analyzed under different experimental conditions of temperature (100 – 500 °C) and stoichiometric quantities of the Nb$_2$O$_5$-KHSO$_4$-H$_2$SO$_4$ system (1:2:5 and 1:1:2.5 mol:mol:mol). In this stage, the formation of Nb sulfate products was evaluated by minimizing the Gibbs free energy for the input compositions. Due to insufficient thermodynamic data for Ta, thermodynamic simulations could not be performed.

2.3.3. Acid roasting

The ground sample was sieved to a particle size smaller than 75 μm to ensure a uniform particle size distribution. For the roasting tests, 5 g of the slag powder was mixed uniformly with potassium bisulfate (KHSO4) in a porcelain crucible. An appropriate amount of concentrated sulfuric acid (H2SO4) was added, and the mixture was homogenized to ensure contact between the reagents and the original sample. The

porcelain crucible with the sample was then transferred to a muffle furnace previously heated at a rate of 10 °C/min until the ideal temperature of 300 °C was reached. Once the furnace reached the predetermined temperature, the sample was maintained for 120 min. After roasting, the crucible was removed from the furnace, and the roasted material was cooled to room temperature.

2.3.4. Leaching

The leaching tests were conducted in 250 ml Erlenmeyer flasks on an orbital shaker. The leaching solutions were prepared in volumetric flasks and transferred to the Erlenmeyer flasks for conditioning on the orbital shaker at the desired temperature. The roasted slag mass was then introduced, and the mixture was agitated continuously (240 rpm) under various controlled experimental conditions, as presented in Table 3. After the experiment, the leached material was allowed to cool to room temperature and filtered using a vacuum pump. EDXRF analyzed the leaching solutions to assess the metal recovery percentage, while the solid residues were dried in an oven for 24 h at 50 °C.

3. Results and discussion

3.1. Characterization of the slag

Fig. 1 shows the results of the mineralogical analysis, indicating that the slag matrix is composed of ZrO$_2$ peaks, which are characteristic of Amazonian soils (Clemente et al., 2023). Additionally, it displays an association of oxides forming the CaOSiO$_2$ phase, which is formed and produced during the carbothermic reduction of cassiterite. This attribution in the results shows homogeneity in the phases, as presented by (Anes et al., 2024; Conrado Da Luz, 2023).

The chemical analysis shown in Table 4 indicates that the elemental concentration in the slag matrix contains 3.86 % Nb and 0.52 % Ta, while the composition of Zr, Si, and Ca elements represents around 40 % of the total slag matrix composition. According to (Anes et al., 2023), 45

Table 3

Evaluation of leaching conditions.

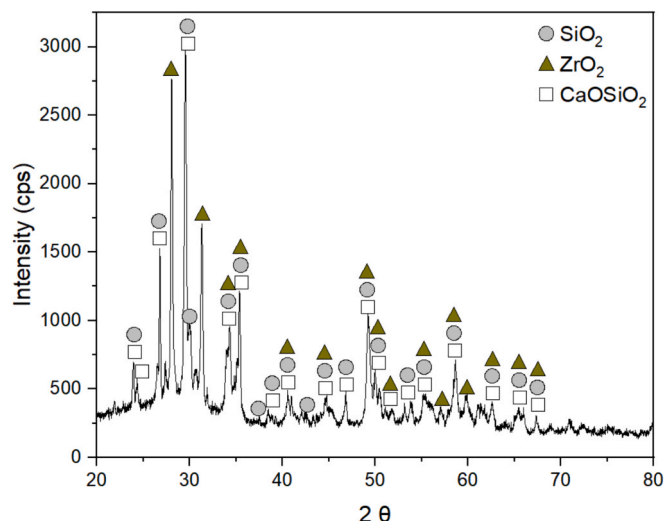| Parameters	Conditions
Solid/liquid ratio (g L^{-1})	20, 40, 50, 66 and 100
Concentration (mol L^{-1})	0.25, 0.5, 0.75, 1 and 2
Temperature (°C)	23, 30, 40, 50 and 60
Time (min)	30, 60, 90, 120 and 180

Fig. 1. X-ray diffraction (XRD) pattern of the tin slag.

Table 4
Chemical analysis of tin slag.

Element	Content (%)	Element	Content (%)
SiO_2	35.5	Hf	1.05
Ca	12.87	Na	0.95
Zr	11.48	Ti	0.87
Nb	3.86	Ta	0.52
Fe	3.34	Zn	0.51
Al	2.4	U	0.5
Sn	2.07	Mn	0.49
Mg	1.91	Y	0.18
Th	1.85	In	0.15
K	1.09	Ba	0.13

% of the total tin slag comprised Si, Ca, and Zr, while Nb and Ta represented only 4 % and 0.5 %, respectively.

3.2. Thermodynamic simulation

The thermodynamic evaluation focused primarily on Nb species due to the availability of reliable data (Cheje Machaca et al., 2025). In the

case of Ta, the lack of consistent thermodynamic data prevented its inclusion in the modeling. (Pourbaix, 1966) demonstrated that the immunity and passivation regions of Ta correspond to the stability domains of its metallic and oxidized forms, indicating high thermodynamic stability and corrosion resistance under specific conditions. Therefore, the experimental results are expected to show behavior similar to that of niobium, given their comparable chemical properties (Deblonde et al., 2019).

Fig. 2 shows the thermodynamic modeling of the Nb_2O_5-$KHSO_4$-H_2SO_4 system to evaluate the Nb sulfated products at different molar ratios. Fig. 2a highlights the formation of $Nb_2O_3(SO_4)_2$ produced by the reaction with H_2SO_4, which stabilizes up to 300 °C due to the decomposition reaction of $KHSO_4$ and H_2SO_4, as shown in Eqs. 1, 2, 3, and 4 (Gao et al., 2021). After this temperature, the reactants decompose, forming $Nb_2O(SO_4)_4$ as the product, produced by the loss of oxygen and substitution by SO_4^{2-} ions, which predominates at temperatures above 300 °C (Wu et al., 2015).

Fig. 2b indicates that an excess in the stoichiometric ratio of the reagents promotes the formation of sulfate products. However, according to the literature, it is documented that increases in the stoichiometric ratio above 0.3 of $KHSO_4$ and over 1.0 of H_2SO_4 in the $KHSO_4$-H_2SO_4-mineral system result in a decrease in extraction rates, leading to unnecessary reagent consumption (Gao et al., 2021). A similar study was conducted by (Gao et al., 2014), who demonstrated that adding an auxiliary sulfate reagent to the H_2SO_4-mineral system when the ratio exceeds 0.5 reduces niobium extraction rates, which aligns with our results.

Our assumption regarding the simulation diagram would be to increase the temperature to 350 °C to favor a higher degree of material conversion and reduce the stoichiometric ratio, as already proposed by (Gao et al., 2021). In this work, focusing on optimizing the parameters, we selected the system ratio of 1:1:2.5 (mol:mol:mol) for the experiments. In terms of working units, this corresponds to 1:0.5:0.5 (g:g:ml).

3.3. Characterization of the roasted material

The roasted product from the Slag-$KHSO_4$-H_2SO_4 system at a molar ratio of 1:0.5:0.5 (g:g:ml) was characterized to follow and understand the sulfation mechanisms of the slag matrix. Fig. 3 shows a characteristic peak of higher intensity referred to as K_2SO_4, which is the product of the addition of $KHSO_4$ and the slag matrix. A peak of $CaSO_4$ was also identified as the product of the chemical reaction with SO_4^{2-} ions, along with the association of unaltered SiO_2-ZrO_2 oxides after the roasting
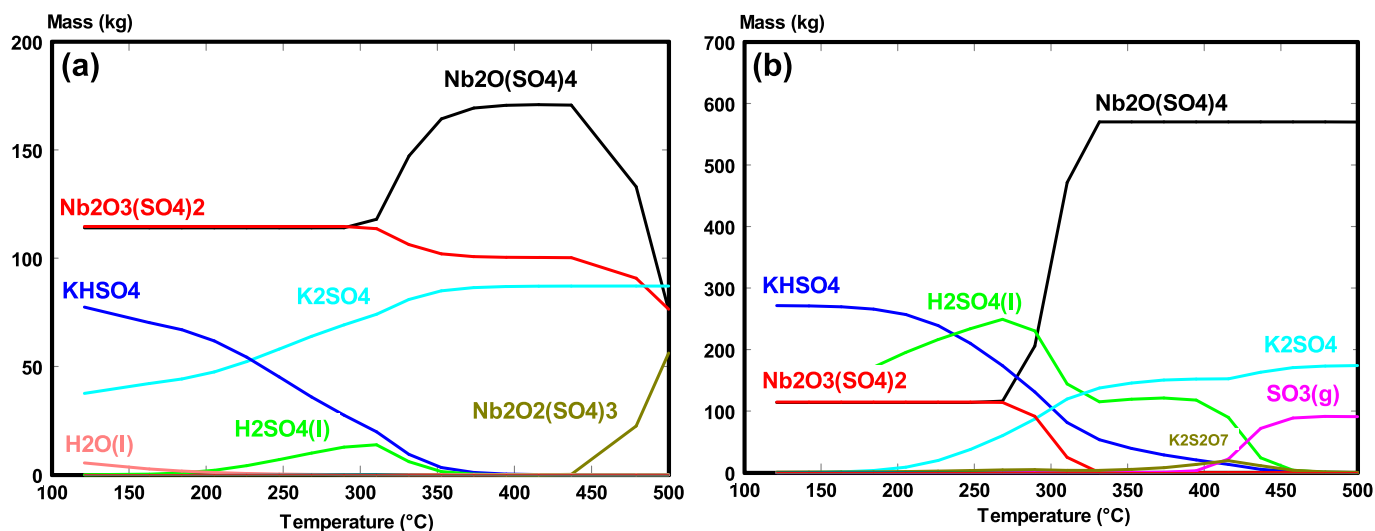

Fig. 2. Thermodynamic simulation of the Nb_2O_5-$KHSO_4$-H_2SO_4 system. (a) 1:1:2.5 M ratio (mol:mol:mol) and (b) 1:2:5 M ratio (mol:mol:mol), performed using HSC v6 software (based on the thermodynamic models of (Cheje Machaca et al., 2025)).
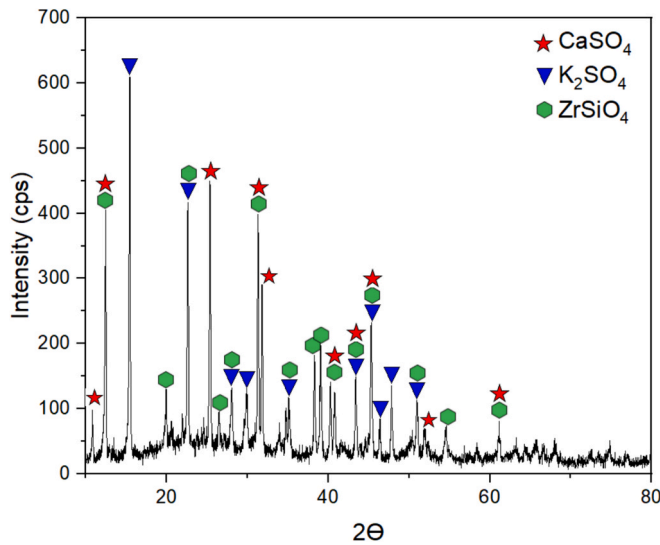
Fig. 3. XRD diffractogram of the roasted material.

process.

Based on the mineralogical study, the chemical composition of the roasted material was analyzed, as shown in Table 5. It can be observed that the product obtained was predominantly composed of K^+ and SO_4^{2-} ions associated with the target metals, resulting from the addition of sulfating reagents. As seen, the roasting process favored the concentration of Nb and Ta due to their release from the original matrix, while other elements such as Ca, Zr, Fe, Al, and Mg showed a significant decrease. In contrast, SiO_2 showed no evidence of any reaction during the process.

3.4. Preliminary test

Some preliminary tests were carried out to compare direct leaching and roasting–leaching under different experimental conditions, as shown in Table 6. Tests **1** and **2** represent direct leaching with sulfuric and oxalic acid, while tests **3** and **4** correspond to the roasted material using the conditions established in the thermodynamic simulation (Fig. 2) and leached with water and sulfuric acid.

Fig. 4 shows a recovery of less than 50 % for Nb and Ta in all experimental tests. Tests number **1** and **2** show that after direct leaching with sulfuric acid, slow kinetics of sulfation and complexation were observed due to the refractory nature and lack of release of the target metals from the silicate matrix. (Deblonde et al., 2019; Pourbaix, 1966)) established the chemical resistance of these metals to inorganic acids, implying the need for thermal processes to improve the solubility of Nb and Ta. In contrast, tests number **3** and **4** showed that after the roasting stage, the formation of soluble metal sulfates increases, which can be hydrolyzed in aqueous media. (Conrado Da Luz, 2023) compared the extraction results of a slag with and without treatment, showing that the roasting process improves metal recovery by up to 50 %.

As can be seen, despite the thermal treatment applied in tests **3** and **4**, metal recovery does not exceed 50 %. It appears that, after the roasting stage, the improvement in metal efficiency is primarily concentrated in the leaching step. (Conrado Da Luz, 2023) evaluated the leaching of a thermally pretreated sample using eight different reagents, highlighting oxalic acid as the most effective in the extraction of Nb and

Table 6
Experimental conditions of the preliminary tests.

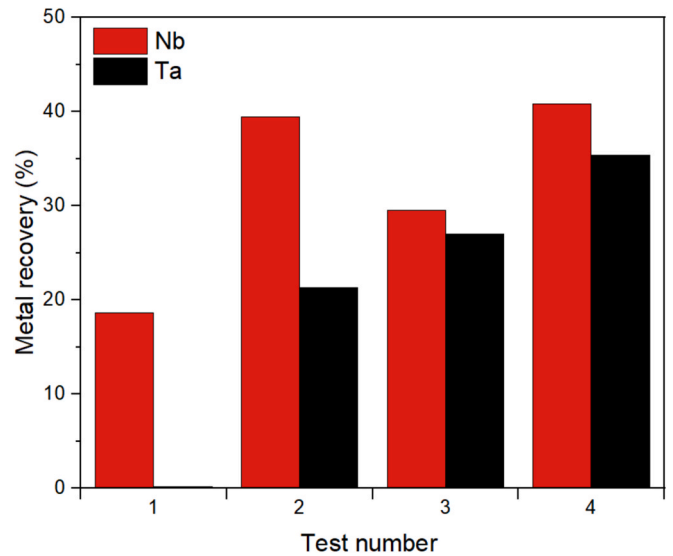| Test	Experimentals conditions Roasting	Leaching
1	–	H_2SO_4 3 M, S/L ratio 1:20, 90 °C, 1 h
2	–	$H_2C_2O_4$ 0,5M, S/L ratio 1:20, 90 °C, 1 h
3	Slag-$KHSO_4$-H_2SO_4 1:0,5:0,5, 300 °C, 2 h	H_2O, S/L ratio 1:20, 90 °C, 1 h
4	Slag-$KHSO_4$-H_2SO_4 1:0,5:0,5, 300 °C, 2 h	H_2SO_4 3 M, S/L ratio 1:20, 90 °C, 1 h

Fig. 4. Comparative evaluation of metal recovery in preliminary tests.

Ta. This trend had already been established by (Pourbaix, 1966), who demonstrated that a pretreated sample in the presence of complexing agents exhibits greater solubility. Based on this background and the conditions already established for the roasting process, the next stage of this study focuses on the solubilization of the roasted material using oxalic acid.

3.5. Leaching

3.5.1. Effect of the solid-liquid ratio

After the roasting process under a 1:0.5:0.5 (g:g:ml) slag-$KHSO_4$-H_2SO_4 ratio at 300 °C for 2 h, the metallic recovery was evaluated during the leaching stage. Fig. 5 shows that increasing the leaching solution results in higher metallic recoveries, as there is greater availability of the $C_2O_4^{2-}$ ion to form the complexes $[NbO(C_2O_4)_3]^{3-}$ and $[TaO(C_2O_4)_3]^{3-}$ (Cheje Machaca et al., 2025). Thus, with a lower ratio of 50 g L^{-1}, recoveries are around 80 %. Although the metallic recoveries are attractive, they are economically unfeasible on an industrial scale due to the large volumes of effluent generated. On the other hand, ratios above 50 g L^{-1} decrease the material's conversion degree and may increase the co-dissolution of undesired elements, such as Ca, from the matrix (Shikika et al., 2022). However, (Brnicevic & Djordjevic, 1968) pointed out the need for stoichiometric ratios up to 10 times for metal solubilization. Our assumption in this regard was to select the 50 g L^{-1} ratio for

Table 5
Chemical composition of the roasted material determined by WDXRF.

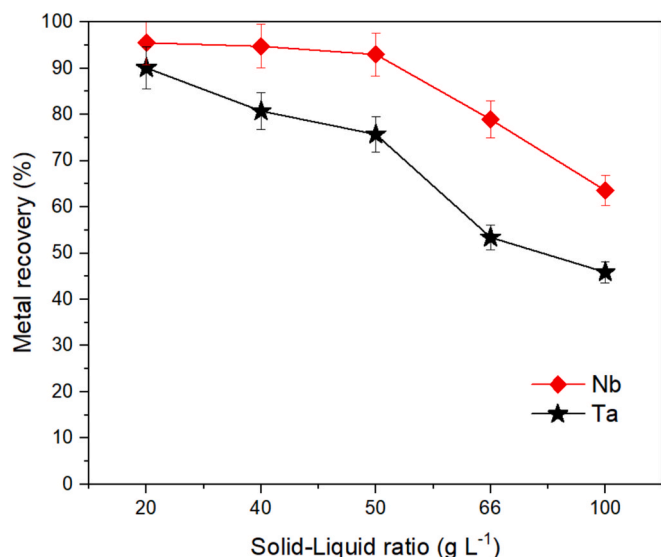| Element	SO₄	SiO₂	ZrO₂	CaO	Nb₂O₅	Fe₂O₃	Al₂O₃	K₂O	MgO	Ta₂O₅
%w/w	28.1	35.4	14.35	10.6	5.8	4.28	3.41	3.95	2.3	0.62

Fig. 5. Effect of the Solid-Liquid ratio on the leaching of Nb and Ta under conditions: 0.5 mol L^{-1}, 60 °C, 60 min.

our subsequent experiments.

3.5.2. Effect of concentration

Fig. 6 shows the variation in concentration from 0.25 to 2 mol L^{-1} during the leaching stage, maintaining constant parameters of a S/L ratio of 50 g L^{-1}, 90 °C for 1 h. It can be observed that at concentrations lower than 0.5 mol L^{-1}, metal conversion rates are less than 20 %. This could be due to the lower availability of the oxalate ion, which affects the isoelectric region or acidity, destabilizing the complexes formed by $[NbO(C_2O_4)_3]^{3-}$ and $[TaO(C_2O_4)_3]^{3-}$ (Deblonde et al., 2019). A decrease in niobium recovery is observed at higher concentrations, as the high concentration induces the precipitation of niobium oxalate and oxalic acid in the solution, reducing the metallic recovery (Jehng & Wachs, 1991).

The behavior of Ta appears to be influenced by the concentration, reaching its maximum recovery at 1 mol L^{-1}. This difference in recovery is related to the solubility of Ta in oxalic media, which requires an excess of oxalate to solubilize it (Brnicevic & Djordjevic, 1968). In this study, a
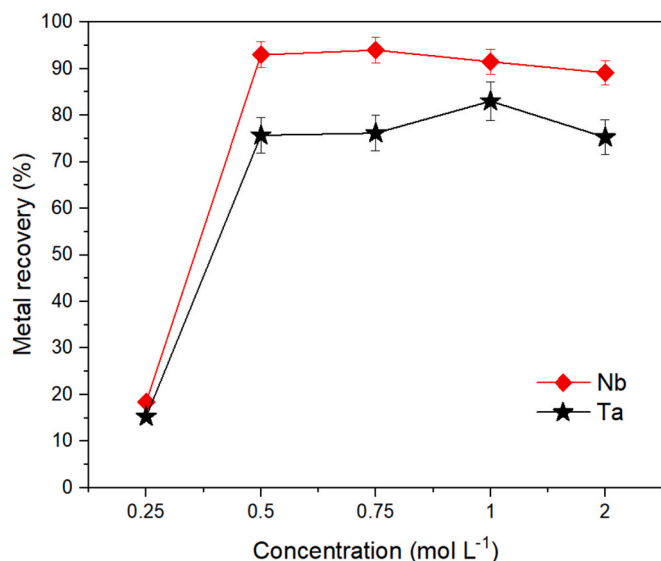
concentration of 0.5 mol L^{-1} was used to reduce the amount of leaching reagent, as proposed in other research works (Conrado Da Luz, 2023; Deblonde et al., 2019).

3.5.3. Effect of temperature

Fig. 7 shows the variation from 23 °C to 60 °C in leaching while maintaining constant parameters of S/L ratio 50 g L^{-1}, 0.5 mol L^{-1} for 1 h. It is documented that temperature favors the reaction kinetics between the involved products (Faraji et al., 2022; Shikika et al., 2022). However, in this study, it is possible to observe that temperature causes two effects: With the increase in temperature, there is a 10 % increase in Nb recovery. In contrast, Ta recovery decreases, possibly due to the susceptibility of oxalates to decompose with the temperature rise. This behavior of metal recovery is similar to that reported in the work of (Conrado Da Luz, 2023).

3.5.4. Effect of leaching time

The effect of leaching time was examined over a range from 25 to 180 min, maintaining constant parameters of S/L ratio 50 g L^{-1}, 0.5 mol L^{-1} at 60 °C. Fig. 8 shows the recovery of our metals at shorter reaction times, and no significant variation is observed with longer durations. In our setup, it is evident that only 30 min are required for the complexation process. Previous studies (Conrado Da Luz, 2023; Gao et al., 2021; Shikika et al., 2022) have shown that after a thermal treatment process, leaching time is not a key variable, as the process focuses on the solubilization of the roasted material. Therefore, a reaction time of 60 min was selected as a reasonable option.

In addition to the parameters studied at their different levels, this study did not address variables such as agitation, which enhances the mass transfer of suspended particles, or particle size, which reduces the boundary layer due to the increased surface area in contact with the liquid (Faraji et al., 2022). These factors could influence the metal recovery.

For the leaching residues, the X-ray diffraction analysis of the leached material, which includes the two stages: acid roasting (1:0.5:0.5 mol:mol:mol, 300 °C for 2 h) and oxalic leaching (0.5 mol L^{-1}, 50 g L^{-1}, 60 °C for 60 min), is shown in Fig. 9. A new peak appears in contrast to the peaks found in the roasting and material characterization diffractograms. In this stage, insoluble oxalate salts such as $CaC_2O_4 \cdot H_2O$ were identified, as noted in previous studies (Conrado Da Luz, 2023; Shikika et al., 2022). Meanwhile, after the entire process, the permanent insoluble phases of SiO_2 and ZrO_2 are observed in the final product.
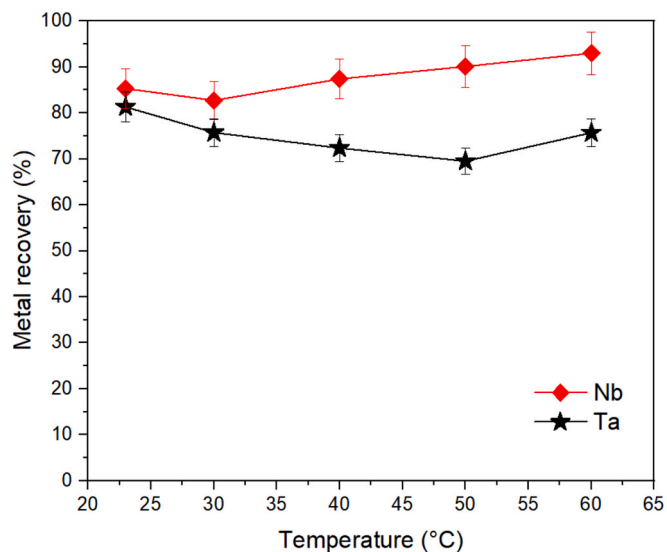

Fig. 6. Effect of organic agent concentration on the leaching of Nb and Ta under conditions: 50 g L^{-1}, 60 °C, 60 min.

Fig. 7. Effect of temperature on Nb and Ta recovery under conditions: 0.5 mol L^{-1}, 50 g L^{-1}, 60 min.
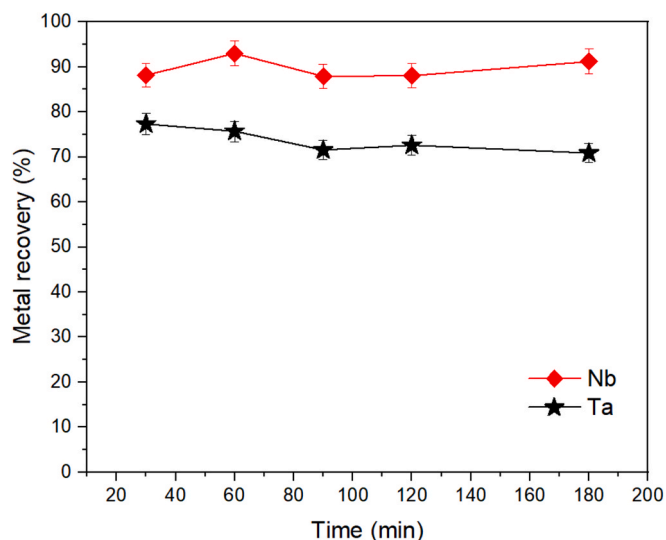
Fig. 8. Effect of time on the leaching of Nb and Ta under conditions: 0.5 mol L^{-1}, 50 g L^{-1}, 60 °C.
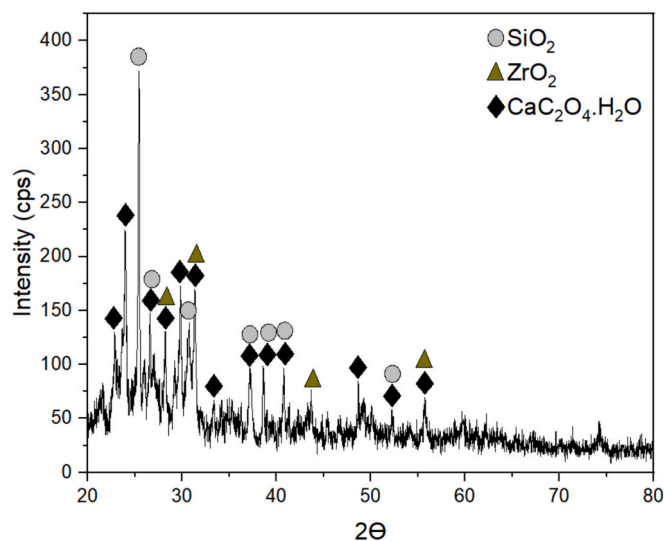

Fig. 9. X-ray diffraction (XRD) pattern of the oxalic leaching residue.

Table 7 presents the chemical analysis of the residue resulting from leaching with oxalic acid. It is observed that, after roasting, the sulfated compounds undergo hydrolysis in aqueous medium, and leaching with oxalic acid favors the formation of stable complexes in solution (Deblonde et al., 2019; Edmister & Albritton, 1932; Fairbrother & Taylor, 1956). In comparison with the roasting data (Table 5), a reduction is evident in the residue content of 0.6 % SO$_4$, 0.8 % K$_2$O, 0.34 % Nb$_2$O$_5$, and 0.16 % Ta$_2$O$_5$. In contrast, a high concentration of ZrO$_2$ and CaO is maintained, which could be attributed to their accumulation in the residue and the formation of poorly soluble oxalates. The SiO$_2$ content, in turn, remains practically unchanged in the residue.

Based on the results obtained from the leaching residue (Table 7), a metallic reduction can be deduced, so the resulting PLS contains metallic traces. This affects the subsequent separation and purification stages.

According to (Cheje Machaca et al., 2025), a preliminary precipitation step can be applied to reduce metallic impurities based on their solubility constant. For example, it is known that Nb^{+5} and Ta^{+5} can precipitate under acidic conditions (pH < 1.5), while elements such as Fe^{+2} and Al^{+3} precipitate starting from a pH = 3 (Ma et al., 2020). This step is necessary to obtain a PLS enriched in Nb/Ta with a significantly lower concentration of metallic contaminants.

3.6. Morphology and phase transformation

Tables 8, 9, and 10 show the composition of selected regions at different points analyzed by EDS, revealing phase transformations throughout the process. The changes in SEM morphology of the original material, the roasted product, and the leach residue are shown in Fig. 10.

Fig. 10(a) shows an amorphous surface composed of particles with irregular sizes and different color shades, attributed to elements that vary according to their electron density. According to Table 8, **point 1** reveals metallic Sn particles that were not reduced during the pyrometallurgical process due to the high viscosity of the slag produced. At **points 2**, **3**, and **4**, a mixture of silicates was found in all the irregular particles. Meanwhile, fine metallic fractions of Nb and Ta are associated with predominant phases of Zr, Si, and Ca (Conrado Da Luz, 2023).

The SEM image of the roasted product (Fig. 10(b)) shows that the morphology of the slag particles underwent distinctive changes after high-temperature roasting with the KHSO$_4$-H$_2$SO$_4$ system. The originally irregularly shaped particles were transformed into smaller, porous, and lumpy structures, which are beneficial for subsequent leaching stages. This phase transformation is mainly attributed to the formation of soluble and insoluble sulfates (Table 9). **Points 1, 2, 3,** and **4** reveal a significant reduction in Nb and Ta content, possibly due to a salt layer on their surface, and an increase in S and K content following the addition of the reagents, confirming the effective decomposition of the original matrix. On the other hand, the EDS data indicate, in all selected points, the presence of silicates and the formation of CaSO$_4$ salts, which partially hinder the sulfating action of the reagents on the matrix. This partially explains the deficiency observed in the recovery of the target metals.

In contrast to the morphology of the original material and the roasted product, it is evident that particle size decreased throughout the process stages, containing traces of soluble sulfates. The SEM image of the leach residue (Fig. 10(c)) shows a reduction in porous particles, indicating that most of the soluble sulfates were dissolved in the leaching solution. Table 10 shows that in all selected points, the sulfur content decreased considerably, while the carbon content increased significantly due to the addition of C$_2$O$_4^{2-}$ ions, forming soluble and insoluble oxalates. Likewise, in the residue, **points 2** and **3** reveal particles with high contents of Ca and Si, respectively, indicating that some particles may not have decomposed during the process.

3.7. Economic feasibility

To assess the economic feasibility of the proposed process, the analysis considered the cost of chemical inputs, electrical energy consumption, and the potential economic benefit of the process.

3.7.1. Cost of chemical reagents

As shown in Table 11, during the process, chemical reagents with an estimated value of 0.547 R\$ (0.071 USD) were used for the treatment of 5 g of sample, with the majority of the cost originating from oxalic acid (70.4 %). This indicates that, although the unit price of KHSO$_4$ is 27.52

Table 7
Chemical composition of the leach residue determined by WDXRF.

Element	SO$_4$	SiO$_2$	ZrO$_2$	CaO	Nb$_2$O$_5$	Fe$_2$O$_3$	Al$_2$O$_3$	K$_2$O	MgO	Ta$_2$O$_5$
%w/w	0.6	32.7	22.7	20.4	0.34	5.53	1.9	0.8	1.04	0.16

Table 8
EDS analysis of the tin slag.

Spot	Element (%w/w)									
	O	Si	Ca	Zr	Nb	Ta	Al	Fe	Mg	Sn
1	79.0	–	5.4	0.1	0.5	1.0	0.8	0.8	1.0	10.4
2	74.8	4.0	7.5	2.1	5.6	1.8	–	–	0.9	–
3	60.1	8.2	8.7	1.8	8.2	3.1	1.8	1.3	1.2	–
4	71.0	10.7	4.2	0.3	–	4.3	–	3.9	1.7	–

Table 9
EDS analysis of the roasted material.

Spot	Element (%w/w)									
	O	Si	Ca	Zr	K	C	Al	Fe	Mg	S
1	47.0	6.8	7.2	1.7	8.5	6.7	2.5	3.5	1.3	14.7
2	52.9	4.1	4.8	3.8	3.5	9.9	1.8	3.7	1.6	12.9
3	53.3	2.7	3.2	–	6.0	6.5	1.7	6.2	2.5	16.7
4	57.1	5.9	6.0	3.4	2.1	6.7	2.2	2.6	1.7	12.3

Table 10
EDS analysis of the leach residue.

Spot	Element (%w/w)									
	O	Si	Ca	Zr	K	C	Al	Fe	Mg	S
1	57.1	5.6	2.6	–	–	13.1	21.6	–	–	–
2	64.4	0.8	13.8	3.9	–	16.9	0.3	–	–	–
3	61.2	14.6	2.9	–	0.4	15.1	2.6	1.7	0.7	0.3

USD/kg and the unit price of oxalic acid is lower (7.972 USD/kg), its higher consumption in the process increases its economic impact, surpassing that of bisulfate and sulfuric acid. Therefore, this result suggests that it would be advisable to carry out further studies on the efficiency and optimization of process parameters in order to reduce oxalic acid consumption, as it is a green reagent still maturing as an alternative to conventional processes.

3.7.2. Electrical consumption cost

Table 12 presents the estimated energy cost associated with the experimental process developed in this study. In this work, a value of R$ 0.656 per kWh was considered, corresponding to the year 2024 in Brazil, which is approximately equivalent to 0.12 USD (Salazar et al., 2024). The process consisted of the size reduction stage, acid roasting, and leaching, with a total energy cost of 0.699 USD. We found that, to maintain a temperature of 300 °C inside the furnace, a power of 2.2 kWh was extracted, which, when multiplied by the operating time of 2 h and the energy cost, resulted in a cost of 0.52 USD. Meanwhile, the leaching stage at a temperature of 60 °C for 1 h resulted in 0.42 USD, and the size reduction stage only required 2.5 % of the total energy cost of the process.

3.7.3. Economic benefits

The economic benefits of the proposed process were estimated considering the treatment of one ton of slag, as presented in Table 13. It can be observed that after the leaching process under the best-established conditions, 36.4 kg of Nb and 4 kg of Ta are obtained in the leachate, with a combined loss of 1.3 kg compared to the initial metal content. Considering the average prices in 2024 for Nb_2O_5 (59 USD/Kg, (Statista, 2024)) and Ta_2O_5 (170 USD/Kg, (Metals and Ltd 2023), and after converting the metal masses to their corresponding oxides, a total economic value of 3890 USD per ton processed is estimated. This value does not consider the economic cost of other elements present in the matrix, but it highlights the potential economic benefit of the process for the metallurgical industry.

3.8. Environmental and process aspects

Based on the results mentioned above, this process can significantly reduce the number of steps, production costs, and energy consumption compared to previously proposed methodologies (Conrado Da Luz, 2023; Shikika et al., 2022). While this method represents a less aggressive alternative than the use of hydrofluoric acid, the process still requires environmental mitigation measures to ensure compliance with current regulations. From an environmental perspective, roasting with sulfuric acid may generate contrasting opinions due to the production of gaseous emissions, mainly sulfur compounds (SO_x) resulting from the acid decomposition shown in Fig. 2. These emissions can be reduced when operating below the acid's boiling point (<330 °C), producing losses of less than 50 g per mole in the Nb_2O_5-H_2SO_4 system (Cheje Machaca et al., 2025), or emissions can be treated through gas purification systems (Zhang et al., 2014). Leaching residues can be used as strategic resources for metal recovery, such as Zr and Hf, which represent 12.5 % of the initial composition, exceeding the target metals. (Conrado Da Luz, 2023) showed that after oxalic acid leaching, only 10 % of Zr and 3 % of Hf are extracted, with 90 % and 97 % of Zr and Hf respectively remaining in the final residue. These metals from the residues can be extracted via sulfate routes by increasing the acid proportion or varying the electrochemical potential (Cheje Machaca et al., 2025). This opens opportunities in metallurgy for the recovery of high-value metals, promoting the reuse and circularity of residues.

On the other hand, the PLS (pregnant leach solution) generated from this process can be directed to a separation and purification stage, yielding high-purity products. It is documented in the literature that Nb and Ta can be extracted from oxalic acid solutions in sulfuric acid-oxalic acid systems (Djordjević et al., 1966) or from oxalic acid-hydrochloric acid mixtures (Strelow et al., 1972). However, the characteristics of these metals and their halogenated chemistry result in difficult and complex processes that require special conditions. Recently, an emerging versatile technique is ion exchange, which could be applied to the PLS obtained from this process. According to (de Souza Gonçalves et al., 2023), this process can achieve adsorption rates of 63 % for Nb and 78 % for Ta, emerging as an alternative in the extraction process.
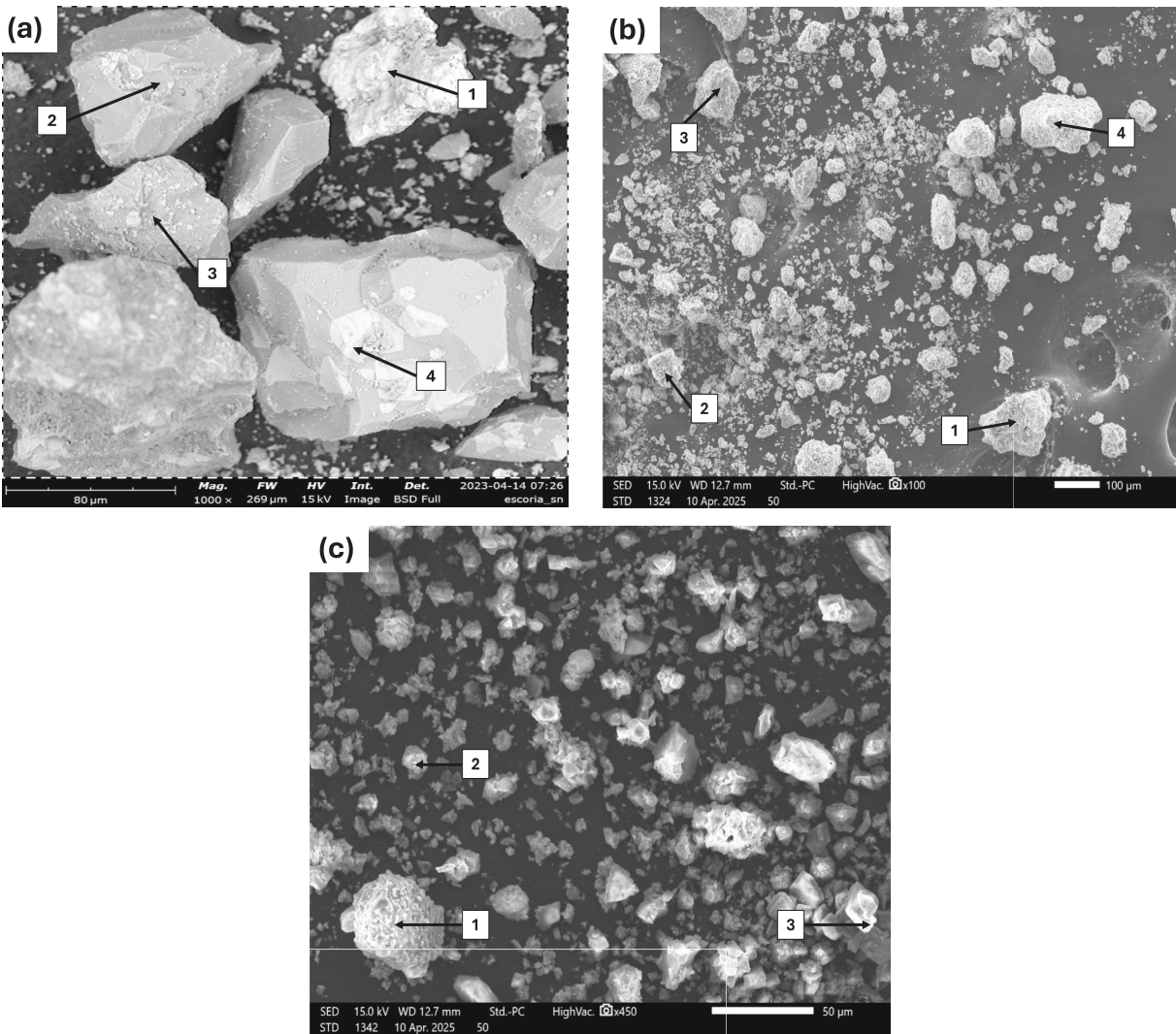
Fig. 10. SEM images of **(a)** tin slag, **(b)** slag roasted with the Slag-KHSO$_4$-H$_2$SO$_4$ system (1:0,5:0,5), and **(c)** leaching residue with H$_2$C$_2$O$_4$.

Table 11
Cost of the chemical reagents used in the process.

Chemical reagent	Unit cost in R$	Cost in USD	Required consumption amount	Total cost R$	Total cost USD
H$_2$SO$_4$	94.53/L	17.34/L	0.5[a]	0.047	0.008
KHSO$_4$	150.0/Kg	27.52/Kg	0.5[b]	0.227	0.013
H$_2$C$_2$O$_4$	43.45/Kg	7.972/Kg	6.3[b]	0.273	0.05
Total cost				0.547	0.071

Note: The cost of the chemical reagents is based on an exchange rate of 1 USD = 5.4501 R$. **a** = Volume (ml), **b** = mass (g).

Therefore, for a more comprehensive evaluation of the environmental impact, a life cycle analysis (LCA) of the process would be necessary, as the newly developed process has a broader application perspective due to the advantages already described.

4. Conclusions

Fig. 11 summarizes the procedure and steps described in this article, based on an alternative approach that consists mainly of two units for processing tin slags without the need for hydrofluoric acid. It was

Table 12
Electricity consumption in the proposed process.

Stage	Temperature (°C)	Operating time (h)	Energy consumption (kWh)	Electricity cost per kWh (USD)
Particle size reduction	–	0.06	2.5	0.018
Acid roasting of slag	300	2	2.2	0.528
Digital control orbital shaker	60	1	1.28	0.153
Total cost				0.699

Table 13
Economic value recovered of Nb and Ta in the leach solution.

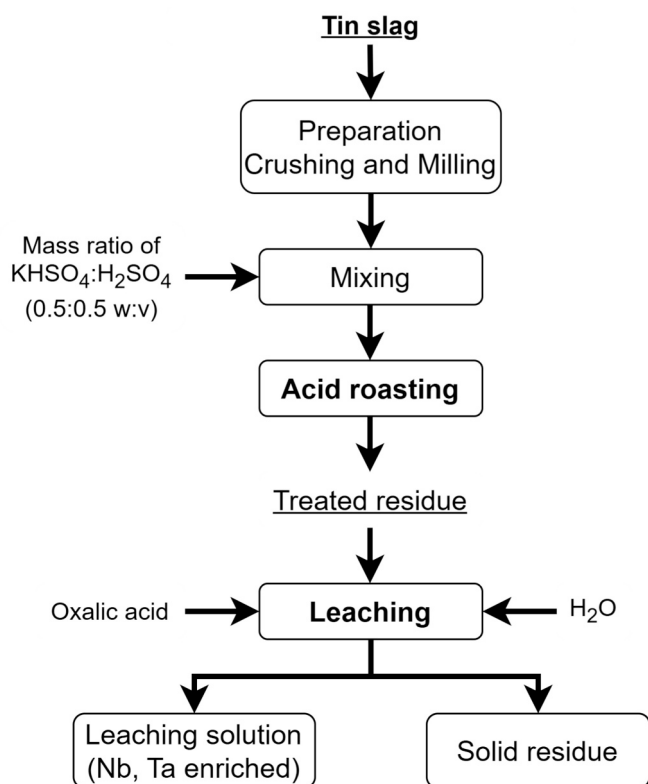| Metal	Mass recovered from leachate (kg)	Metal mass as oxide (kg)	Oxide price (USD/kg)	Recovered oxide value (USD)
Nb	36.4	52.1	59	3074
Ta	4.0	4.8	170	816
Total				3890

Fig. 11. Proposed flowsheet for the recovery of Nb and Ta from tin slags.

determined that the acidic roasting of the Slag-KHSO$_4$-H$_2$SO$_4$ system at a temperature of 300 °C, with a 1:0.5:0.5 (g:g:ml) ratio, particle size of -75 μm, for 2 h, ensures the sulfation of the products through thermodynamic modeling that predicts the optimal working conditions. After the roasting process, the phases were predominantly sulfates and insoluble silicate phases. During the oxalic acid leaching stage, the effects of key operational parameters were studied, resulting in a recovery of 94 % Nb and 75 % Ta, with calcium oxalate, zirconium oxide, and quartz phases remaining in the final leaching residue. These findings represent significant advances in the industrial processing of Nb and Ta from secondary waste, focusing on providing additional benefits in terms of reduced reagent consumption and maximizing the economic potential of the process.

CRediT authorship contribution statement

Darwin Michell Cheje Machaca: Writing – review & editing, Writing – original draft, Visualization, Validation, Project administration, Methodology, Investigation, Formal analysis, Data curation, Conceptualization. **Rosario Belen Juyo Salazar:** Writing – review & editing, Methodology, Data curation. **Thamyres Cardoso de Carvalho:** Writing – review & editing, Project administration, Methodology, Data curation. **Denise Crocce Romano Espinosa:** Visualization, Supervision, Resources, Project administration, Methodology, Funding acquisition, Data curation. **Jorge Alberto Soares Tenório:** Visualization, Supervision, Resources, Project administration, Methodology, Funding acquisition, Data curation, Conceptualization.

Declaration of competing interest

The authors declare that they have no known competing financial interests or personal relationships that could have appeared to influence the work reported in this paper.

Data availability

No data was used for the research described in the article.

References

Abd, M., & Yusof, W. (2005). *Investigating the Potential for Incorporating Tin Slag in Road Pavements* (Issue March) [Nottingham]. https://www.nottingham.ac.uk/research/groups/ntec/documents/theses/wahabsphdthesis.pdf.

Akli, H.F., Permana, S., Maksum, A., Soedarsono, J.W., Widana, K.S., Anggraini, M., Munir, B., 2019. Enrichment of tantalum and niobium contents in bangka tin slag by NaOH and H3PO4Leaching. IOP Conf. Ser.: Mater. Sci. Eng. 547 (1), 012050. https://doi.org/10.1088/1757-899X/547/1/012050.

Allain, E., Kanari, N., Diot, F., Yvon, J., 2019. Development of a process for the concentration of the strategic tantalum and niobium oxides from tin slags. Miner. Eng. 134, 97–103. https://doi.org/10.1016/J.MINENG.2019.01.029.

Anes, I.A., 2023. Lixiviação de nióbio contido em resíduo da produção de estanho. Biblioteca Digital De Teses e Dissertações Da Universidade De São Paulo.

Anes, I.A., Garjulli, F., de Carvalho, M.S., Tenório, J.A.S., Espinosa, D.C.R., Coleti, J.L., 2023. Extraction of niobium in one step from tin slag by NH4F-HCl leaching process. Can. J. Chem. Eng. https://doi.org/10.1002/CJCE.25046.

Anes, I.A., Garjulli, F., Siqueira de Carvalho, M., Tenório, J.A.S., Espinosa, D.C.R., Coleti, J.L., 2024. Extraction of niobium in one step from tin slag by NH4F-HCl leaching process. Can. J. Chem. Eng. 102 (1), 168–176. https://doi.org/10.1002/CJCE.25046.

Brnicevic, N., Djordjevic, C., 1968. Coordination complexes of niobium and tantalum. VI. Seven-coordinated oxalatoniobates(V) and -tantalates(V). Inorg. Chem. 7 (9), 1936–1938. https://doi.org/10.1021/ic50067a054.

Brocchi, E.A., Moura, F.J., 2008. Chlorination methods applied to recover refractory metals from tin slags. Miner. Eng. 21 (2), 150–156. https://doi.org/10.1016/J.MINENG.2007.08.011.

Calvo, G., Valero, A., 2022. Strategic mineral resources: Availability and future estimations for the renewable energy sector. Environ. Development 41, 100640. https://doi.org/10.1016/j.envdev.2021.100640.

Cheje Machaca, D.M., de Carvalho, T.C., Soares Tenório, J.A., Romano Espinosa, D.C., 2025. Advancements in the extraction of niobium and tantalum: innovative strategies in hydrometallurgical processes. Miner. Eng. 222, 109125. https://doi.org/10.1016/j.mineng.2024.109125.

Clemente, D.M., da Silva, C.A., Peixoto, J.J.M., de Oliveira, J.R., de Souza, R.M., 2023. Investigation of the presence of metallic phases in brazilian tin-slags. J. Mater. Res. Technol. 24, 6861–6875. https://doi.org/10.1016/J.JMRT.2023.04.251.

Conrado Da Luz, V. (2023). *Extração de nióbio e tântalo contidos na escória da produção de estanho por lixiviação em ácido oxálico* [Universidade de São Paulo]. https://doi.org/10.11606/D.3.2023.tde-21112023-150803.

de Oliveira, T.F., de Souza, C.P., Lopes-Moriyama, A.L., 2020. Acid leaching and thermal treatments in the obtaining of mixed oxides of Nb and Ta from ferrocolumbite. Miner. Eng. 147, 106157. https://doi.org/10.1016/J.MINENG.2019.106157.

de Souza Gonçalves, G.A., de Carvalho, T.C., Garjulli, F., de Carvalho, M.S., Espinosa, D. C.R., 2023. Adsorption of niobium and tantalum contained in a tin slag leachate by ion exchange resins: equilibrium isotherms, kinetic and thermodynamic studies. J. Sustain. Metallurgy 9 (3), 1329–1343. https://doi.org/10.1007/s40831-023-00722-0.

Deblonde, G.-J.-P., Bengio, D., Beltrami, D., Bélair, S., Cote, G., Chagnes, A., 2019. Niobium and tantalum processing in oxalic-nitric media: Nb2O5·nH2O and Ta2O5·nH2O precipitation with oxalates and nitrates recycling. Sep. Purif. Technol. 226, 209–217. https://doi.org/10.1016/j.seppur.2019.05.087.

Djordjević, C., Goričan, H., Tan, S.L., 1966. Solvent extraction of niobium and tantalum: III. Extraction mechanism in oxalic solutions with longchain tertiary amines. J. Less Common Metals 11 (5), 342–350. https://doi.org/10.1016/0022-5088(66)90066-X.

DOE. (2023). *Critical Materials Assessment* (Issue July). https://www.energy.gov/eere/articles/us-department-energy-releases-2023-critical-materials-assessment-evaluate-supply.

Dutta, S. K., & Lodhari, D. R. (2018). *Extraction of Nuclear and Non-ferrous Metals*. Springer Singapore. https://doi.org/10.1007/978-981-10-5172-2.

Edmister, F.H., Albritton, G.G., 1932. Behavior of oxalate and tartrate solutions of columbium and tantalum oxides1. J. Am. Chem. Soc. 54 (2), 438–442. https://doi.org/10.1021/ja01341a004.

European Commission. (2023). *Study on the Critical Raw Materials for the EU 2023 - Final Report*. https://doi.org/10.2873/725585.

Fairbrother, F., Taylor, J.B., 1956. 961. Water-soluble complexes of niobium (columbium) and tantalum. Part I. Complexes with α-hydroxy-acids and (2-hydroxyethyl)-amines. J. Chem. Soc. (Resumed) 4946–4954. https://doi.org/10.1039/JR9560004946.

Faraji, F., Alizadeh, A., Rashchi, F., Mostoufi, N., 2022. Kinetics of leaching a Review. 38 (2), 113–148. https://doi.org/10.1515/revce-2019-0073.

Gao, W.C., Wen, J.K., Wu, B., Shang, H., 2014. Extraction of niobium, yttrium, and cerium from a low-grade niobium-bearing ore by roasting (NH4)2SO4-Na2SO4-H2SO4 system. Rare Met. 33 (6), 754–760. https://doi.org/10.1007/S12598-014-0371-7/FIGURES/10.

Gao, W.C., Wen, J.K., Wu, B., Shang, H., Liu, X., 2021. A novel approach to extract Nb, Y and Ce from a niobium-bearing ore of low grade by roasting KHSO4–H2SO4 system. Rare Met. 40 (7), 1979–1986. https://doi.org/10.1007/S12598-020-01435-Z/TABLES/5.

Garcia, M. A. A. (2009). Caracterização Radioquímica e Impacto Radiológico Ambiental no Processamento de Cassiterita para a Produção de Estanho e Chumbo Metálicos [Instituto de Pesquisas Energéticas e Nucleares …]. https://pdfs.semanticscholar.org/d9fe/12ee003f1edac5ec4e248c32336947e35644.pdf.

Globe Metals & Mining Ltd. (2023). *Carbochlorination vs HF/SX: The impact on the environment.* https://www.linkedin.com/company/globe-metals-mining-ltd/posts/?feedView=all.

Jehng, J.-M., Wachs, I.E., 1991. Niobium oxide solution chemistry. J. Raman Spectrosc. 22 (2), 83–89. https://doi.org/10.1002/JRS.1250220207.

Kim, J., Azimi, G., 2020. Technospheric mining of niobium and titanium from electric arc furnace slag. Hydrometall. 191, 105203. https://doi.org/10.1016/j.hydromet.2019.105203.

López, F. A., García-Díaz, I., Largo, O. R., Polonio, F. G., & Llorens, T. (2018). Recovery and Purification of Tin from Tailings from the Penouta Sn–Ta–Nb Deposit. *Minerals 2018, Vol. 8, Page 20*, 8(1), 20. https://doi.org/10.3390/MIN8010020.

Ma, Y., Stopic, S., Wang, X., Forsberg, K., & Friedrich, B. (2020). Basic Sulfate Precipitation of Zirconium from Sulfuric Acid Leach Solution. *Metals 2020, Vol. 10, Page 1099*, 10(8), 1099. https://doi.org/10.3390/MET10081099.

Mikhail, S.A., Webster, A.H., 1992. Recovery of nickel, cobalt and copper from industrial slags—I. Extraction into iron sulphide matte. Can. Metall. Q. 31 (4), 269–281. https://doi.org/10.1179/cmq.1992.31.4.269.

Oliveira, J. M. de. (2022). *ESTUDO DE ROTA HIDROMETALÚRGICA PARA EXTRAÇÃO DE NIÓBIO E TANTALO CONTIDOS NA ESCÓRIA DE ESTANHO* [São Paulo]. https://doi.org/10.11606/D.3.2022.tde-05072023-101320.

Permana, S., Abdul Majid, R., Wahyuadi Soedarsono, J., 2020. Hydrochloric acid leaching approaches for tantalum and niobium pentoxides enrichment in 1st tin slag from bangka island. IOP Conf. Ser.: Mater. Sci. Eng. 924 (1), 012025. https://doi.org/10.1088/1757-899X/924/1/012025.

Pope, N., & Smith, P. (2023). *BRAZIL'S CRITICAL AND STRATEGIC MINERALS IN A CHANGING WORLD.* https://igarape.org.br/en/brazils-critical-and-strategic-minerals-in-a-changing-world/.

Pourbaix, M., 1966. Atlas of electrochemical equilibria in aqueous solutions. NACE.

Research and Markets. (2024). Mining Waste Management Market Report: Mining Waste Management Market by Mining Type, Mineral/Metal Type, Waste Type, and Region -

Global Forecast to 2027. https://www.researchandmarkets.com/reports/5768976/mining-waste-management-market-report-mining#src-pos-2.

Rodríguez, O., Alguacil, F.J., Baquero, E.E., García-Díaz, I., Fernández, P., Sotillo, B., López, F.A., 2020. Recovery of niobium and tantalum by solvent extraction from Sn–Ta–Nb mining tailings. RSC Adv. 10 (36), 21406–21412. https://doi.org/10.1039/D0RA03331F.

Salazar, R.B.J., Tenório, J.A.S., Espinosa, D.C.R., dos Passos Galluzzi Baltazar, M., 2024. Streamlined process with a sustainable approach for photovoltaic module recycling. e01047 Sustain. Mater. Technol. 41. https://doi.org/10.1016/j.susmat.2024.e01047.

Shen, H., Forssberg, E., 2003. An overview of recovery of metals from slags. Waste Manag. 23 (10), 933–949. https://doi.org/10.1016/S0956-053X(02)00164-2.

Shikika, A., Zabene, F., Muvundja, F.A., Mugumaoderha, M.C., Aatach, M., Gaydardzhiev, S., 2022. Efficient extraction of Ta and Nb from a coltan ore through alkaline roasting, water leaching, precipitation, and oxalic acid leaching. J. Sustain. Metallurgy 8 (4), 1932–1947. https://doi.org/10.1007/S40831-022-00621-W/FIGURES/12.

Soedarsono, J.W., Permana, S., Hutauruk, J.K., Adhyputra, R., Rustandi, A., Maksum, A., Widana, K.S., Trinopiawan, K., Anggraini, M., 2018. Upgrading tantalum and niobium oxides content in Bangka tin slag with double leaching. IOP Conf. Ser.: Mater. Sci. Eng. 316 (1), 012052. https://doi.org/10.1088/1757-899X/316/1/012052.

Statista. (2024). *Tantalum price 2024.* https://www.statista.com/statistics/1009173/tantalum-price/.

Strelow, F.W.E., Weinert, C.H.S.W., Eloff, C., 1972. Distribution coefficients and anion exchange behavior of elements in oxalic acid-hydrochloric acid mixtures. Anal. Chem. 44 (14), 2352–2356. https://doi.org/10.1021/ac60322a001.

Vincia, S.F., Permana, S., Maksum, A., Soedarsono, J.W., Widana, K.S., Trinopiawan, K., Munir, B., 2019. Study to enhance tantalum and niobium contents in bangka tin slag by NaOH and HClO4 leaching. IOP Conf. Ser.: Mater. Sci. Eng. 547 (1), 012049. https://doi.org/10.1088/1757-899X/547/1/012049.

Wang, G. C. (2016). *3 - Nonferrous metal extraction and nonferrous slags* (G. C. B. T.-T. U. of S. in C. I. C. Wang (ed.); pp. 35–61). Woodhead Publishing. https://doi.org/10.1016/B978-0-08-100381-7.00003-3.

Wu, B., Shang, H., Gao, W.C., Wen, J.K., 2014. Leaching of niobium from low-grade refractory ore using H2SO4 roast system. Adv. Mat. Res. 997, 651–654. https://doi.org/10.4028/WWW.SCIENTIFIC.NET/AMR.997.651.

Wu, B., Shang, H., Wen, J.K., 2015. Sulfuric acid leaching of low-grade refractory tantalum–niobium and associated rare earths minerals in Panxi area of China. Rare Met. 34 (3), 202–206. https://doi.org/10.1007/S12598-014-0436-7/FIGURES/8.

Xie, K., Wei, X., Ye, L., Wan, M., Li, S., & Wu, J. (2022). Recovery and Preparation of Potassium Fluorotantalate from High-Tantalum-Bearing Waste Slag by Pressure Alkaline Decomposition. *Metals 2022, Vol. 12, Page 648*, 12(4), 648. https://doi.org/10.3390/MET12040648.

Zhang, B., Liu, C., Li, C., Jiang, M., 2014. A novel approach for recovery of rare earths and niobium from Bayan Obo tailings. Miner. Eng. 65, 17–23. https://doi.org/10.1016/J.MINENG.2014.04.011.